Astronomy & Astrophysics manuscript no. output
December 10, 2025

Forming localized dust concentrations in a dust ring

DM Tau case study

Hauyu Baobab Liu[1]

Department of Physics, National Sun Yat-Sen University, No. 70, Lien-Hai Road, Kaohsiung City 80424, Taiwan, R.O.C.
e-mail: hyliu.nsysu@mail.nsysu.edu.tw

Received November 25, 2025; accepted November 26, 2025

ABSTRACT

Context. Previous high-angular-resolution 225 GHz (~1.3 mm) continuum observations of the transitional disk DM Tau have resolved an outer ring at 20-120 au radii that is weakly azimuthally asymmetric.
Aims. We aim to examine dust growth and filtration in the outer ring of DM Tau.
Methods. We performed ~0.″06 (~8.7 au) resolution Karl G. Jansky Very Large Array (JVLA) 40–48 GHz (~ 7 mm; Q band) continuum observations, along with complementary observations at lower frequencies. In addition, we analyzed the archival JVLA observations undertaken since 2010.
Results. Intriguingly, the Q band image resolved the azimuthally highly asymmetric, knotty dust emission sources close to the inner edge of the outer ring. Fitting the 8-700 GHz spectral energy distribution (SED) with two dust components indicates that the maximum grain size ($a_{\rm max}$) in these knotty dust emission sources is likely $\gtrsim$300 μm, whereas it is $\lesssim$50 μm in the rest of the ring. These results may be explained by a trapping of inwardly migrating "grown" dust close to the ring inner edge. The exact mechanism for developing the azimuthal asymmetry has not yet been identified, which may be due to planet-disk interaction that might also be responsible for the creation of the dust cavity and pressure bump. Otherwise, it may be due to the fluid instabilities and vortex formation as a result of shear motions. Finally, we remark that the asymmetries in DM Tau are difficult to diagnose from the $\gtrsim$225 GHz observations, owing to a high optical depth at the ring. In other words, the apparent symmetric or asymmetric morphology of the transitional disks may be related to the optical depths of those disks at the observing frequency.

Key words. Protoplanetary disks – Planets and satellites: formation – (ISM:) dust, extinction – Radio continuum: ISM

1. Introduction

2. Data and reduction

2.1. Data

We carried out the JVLA observations towards DM Tau at Q (40–48 GHz), Ku (12–18 GHz), and X (8–12 GHz) bands in 2019.

We performed a ~3″ angular resolution SMA 200–400 GHz survey towards 47 Class II objects in the Taurus-Auriga region in 2021 that included DM Tau as one of the target sources.

We retrieved the archival ALMA Band 3 (~95–111 GHz), Band 4 (~144–159 GHz), and Band 9 (~659–676 GHz) observations that the maximum recoverable angular scales (MAS) are larger than 3″ for the purpose of deriving the (sub)millimeter SEDs.

Finally, to reference the locations of spatially resolved features in the JVLA observations, we utilized the high-angular-resolution ALMA 216–233 GHz images towards DM Tau, which were detailed in Kudo et al. (2018) (c.f. Hashimoto et al. 2021).

2.2. JVLA data processing

We manually calibrated the JVLA data following the standard strategy (see details below) using the CASA software package.

For the Q band (40–48 GHz) observations taken in 2019 (Table **??**), we additionally used the observations on 3C138 to calibrate the cross-hand delay and absolute polarization position angle and we used the observations on J0319+4130 (3C84) to calibrate the polarization leakage (i.e., D-terms).

We performed multi-frequency synthesis (nterms=2) imaging (Rau & Cornwell 2011) using the CASA `tclean` task. For individual epochs of observations, the achieved synthesized beams and root-mean-square (RMS) noise in the Briggs Robust=2.0 weighted images are summarized in Table **??**.

We jointly imaged all C band (4–8 GHz) observations taken in 2011, which yielded a 5.3 μJy beam^{-1} RMS noise.

3. Results

Figure 1 shows a comparison of the Q band (40–48 GHz; ~7 mm) continuum image generated from combining all the observations at >200 kλ uv distances (Q-fiducial image, hereafter) and the ALMA 225 GHz image made at the same synthesized beam (Section 2.1).

The most prominent feature in the ALMA image is a ring at ~25 au radii that is only weakly asymmetric.

In contrast, the JVLA Q band continuum images are dominated by an incomplete ring (Figure 1, right panel).

In the Q-fiducial image (Figure 1), several knots are detected at ~3–6σ level in east to south within the 25 au ring.

Figure 2 shows the 8–700 GHz SED of DM Tau and some upper limits at lower frequencies.

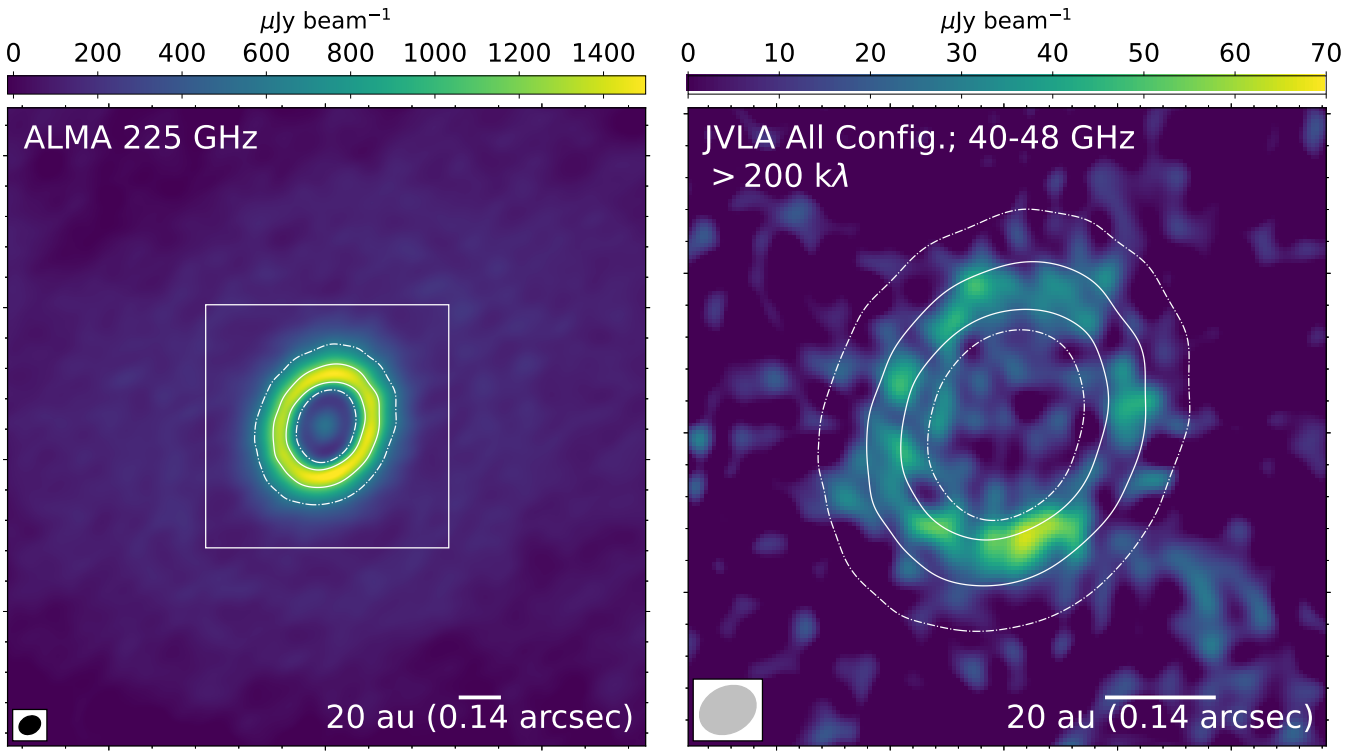

Fig. 1. ALMA and JVLA images on DM Tau. *Left:* Previously published ALMA 225 GHz (∼1.3 mm) continuum image (color and contours; Kudo et al. 2018; Hashimoto et al. 2021) smoothed to the synthesized beam of the JVLA image in the right panel. Dash-dotted and solid contours are 600 and 1200 μJy beam^{-1}, respectively. *Right:* JVLA 40–48 GHz (∼7 mm) continuum image (color; $\theta_{\rm maj} \times \theta_{\rm min}$=0.″074×0.″058, P.A.= −63°; RMS=11 μJy beam^{-1}) in the region enclosed by the white box in the left panel. This image was created by jointly imaging all Q band observations listed in Table **??**, limiting the *uv*-distance to >200 kλ. The images made with other combination of array configurations are provided in Figure **??**. Contours are identical to those plotted in the left panel. The synthesized beams of the ALMA (black) and JVLA images (gray) are plotted in the bottom-left.

4. Discussion

4.1. Spectral index distribution and model

4.2. Physical implications

4.2.1. Asymmetry in protoplanetary disks

Physically, two general ideas have been proposed to explain asymmetries in disk rings.

Phenomenologically, we may also classify sources based on the morphology at 225 GHz and 40–48 GHz.

The DM Tau dusty disk, which appears weakly azimuthally asymmetric and smooth at $\gtrsim$200 GHz and then appears highly asymmetric at $\lesssim$50 GHz, may represent a link between these two kinds.

4.2.2. Dust growth in an initially smooth background disk

5. Conclusion

Acknowledgements. The National Radio Astronomy Observatory is a facility of the National Science Foundation operated under cooperative agreement by Associated Universities, Inc. This paper makes use of the following ALMA data: ADS/JAO.ALMA #2013.1.00498.S, #2013.1.00647.S, #2015.1.00296.S, #2016.1.00565.S., #2016.1.01042.S, #2017.1.01460.S, #2018.1.01755.S. ALMA is a partnership of ESO (representing its member states), NSF (USA) and NINS (Japan), together with NRC (Canada), MOST and ASIAA (Taiwan), and KASI (Republic of Korea), in cooperation with the Republic of Chile. The Joint ALMA Observatory is operated by ESO, AUI/NRAO and NAOJ. The Submillimeter Array is a joint project between the Smithsonian Astrophysical Observatory and the Academia Sinica Institute of Astronomy and Astrophysics, and is funded by the Smithsonian Institution and the Academia Sinica (Ho et al. 2004). H.B.L. is supported by the National Science and Technology Council (NSTC) of Taiwan (Grant Nos. 113-2112-M-110-022-MY3).

References

Chung, C.-Y., Andrews, S. M., Gurwell, M., et al. 2023, Astrophysical Journal Supplement submitted
Hashimoto, J., Muto, T., Dong, R., et al. 2021, ApJ, 911, 5
Ho, P. T. P., Moran, J. M., & Lo, K. Y. 2004, ApJ, 616, L1
Kudo, T., Hashimoto, J., Muto, T., et al. 2018, ApJ, 868, L5
Rau, U. & Cornwell, T. J. 2011, A&A, 532, A71
Terada, Y., Liu, H. B., Mkrtichian, D., et al. 2023, ApJ, 953, 147

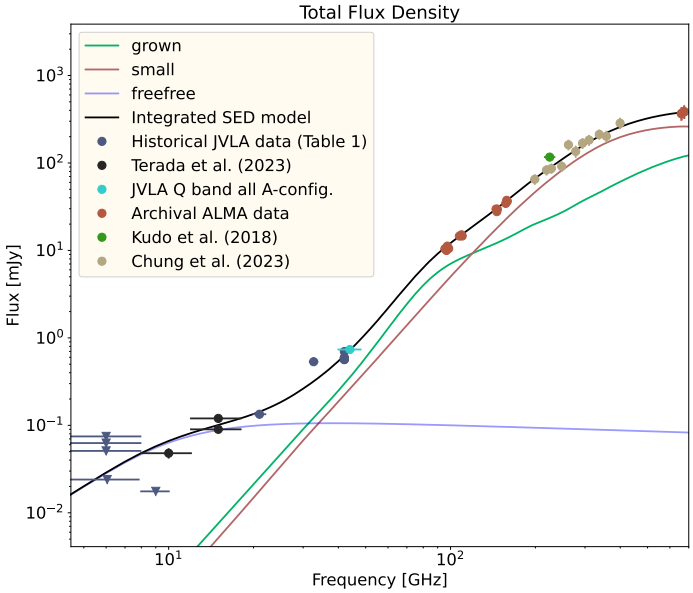

Fig. 2. Flux densities of the DM Tau disk (λ =0.43–67 mm). Dots are the flux density measurements made from our own and the archival JVLA observations (for details see Section 2.1), ALMA 225 GHz measurement from (Kudo et al. 2018), JVLA 8–12 GHz and 12–18 GHz measurements from (Terada et al. 2023), archival ALMA Band 3, 4, and 9 observations (Table **??**), and the SMA 200–400 GHz measurements quoted from Chung et al. (2023). Triangles are the 3-σ upper limits. The vertical error bars $\pm 1\sigma$ error; the horizontal error bars show the frequency coverages of the measurements. The sizes of some symbols are larger than the error bars. Green, red, and blue lines show the flux densities of the grown dust, small dust, and free-free emission components in our best-fit model (Table **??**; Section 4) while the black line shows the integrated flux densities of these models.